AMERICAN ACADEMY OF OPHTHALMOLOGY®

Analysis of the Retinal and Choroidal Vasculature Using Ultrawidefield Fundus Imaging in Mild Cognitive Impairment and Normal Cognition

Suzanna Joseph,[1,2,] Alice Haystead,[2,*] Cason B. Robbins, MD,[1,2] Adam Threlfall, PhD,[4] Tom J. MacGillivray, PhD,[4] Sandra Stinnett, DrPH,[1,2] Dilraj S. Grewal, MD, FASRS,[1,2,**] Sharon Fekrat, MD, FASRS[1,2,3,**]*

Purpose: To utilize ultrawidefield (UWF) imaging to evaluate retinal and choroidal vasculature and structure in individuals with mild cognitive impairment (MCI) compared with that of controls with normal cognition.

Design: Prospective cross sectional study.

Participants: One hundred thirty-one eyes of 82 MCI patients and 230 eyes of 133 cognitively normal participants from the Eye Multimodal Imaging in Neurodegenerative Disease Study.

Methods: A scanning laser ophthalmoscope (California, Optos Inc) was used to obtain UWF fundus color images. Images were analyzed with the Vasculature Assessment Platform for Images of the Retina UWF (VAMPIRE-UWF 2.0, Universities of Edinburgh and Dundee) software.

Main outcome measures: Imaging parameters included vessel width gradient, vessel width intercept, large vessel choroidal vascular density, vessel tortuosity, and vessel fractal dimension.

Results: Both retinal artery and vein width gradients were less negative in MCI patients compared with controls, demonstrating decreased rates of vessel thinning at the periphery ($P < 0.001$; $P = 0.027$). Retinal artery and vein width intercepts, a metric that extrapolates the width of the vessel at the center of the optic disc, were smaller in MCI patients compared with that of controls ($P < 0.001$; $P = 0.017$). The large vessel choroidal vascular density, which quantifies the vascular area versus the total choroidal area, was greater in MCI patients compared with controls ($P = 0.025$).

Conclusions: When compared with controls with normal cognition, MCI patients had thinner retinal vasculature manifested in both the retinal arteries and the veins. In MCI, these thinner arteries and veins attenuated at a lower rate when traveling toward the periphery. MCI patients also had increased choroidal vascular density.

Financial Disclosure(s): Proprietary or commercial disclosure may be found in the Footnotes and Disclosures at the end of this article. *Ophthalmology Science 2024;4:100480*

Supplemental material available at www.ophthalmologyscience.org.

Mild cognitive impairment (MCI) refers to an intermediary state between normal aging and dementia in which patients develop cognitive debility that does not significantly interfere with instrumental activities of daily living.[1] Individuals with MCI carry a significant risk of developing Alzheimer dementia (AD).[1,2] Referral clinic studies have found that MCI patients progress to AD at rates of 10% to 15% per year, with 80% converting to AD within 6 years.[3,4] This highlights the need for close monitoring of MCI patients for progression to AD. Earlier identification may allow for the implementation of treatments before the progression of cognitive decline. However, MCI is currently a clinical diagnosis characterized by a decline in memory and daily cognitive function from baseline.[5] As such, physicians are reliant on caretaker reports to obtain an accurate representation of the patient's prior intellectual function and development of new deficits.[5] Given multiple challenges inherent to making the diagnosis and characterizing MCI, physicians are now turning toward quantitative markers of disease, such as image-based and cerebrospinal fluid-based biomarkers, the most promising of which include measurement of cerebrospinal fluid levels of amyloid β-40, amyloid β-42, total τ, and phosphorylated τ.[6,7] However, obtaining such biomarkers is invasive, expensive, and, often, not widely accessible.

There has been increasing interest in the identification of ophthalmic biomarkers for neurodegenerative disease.[8–11] As an extension of the central nervous system, the retina

https://doi.org/10.1016/j.xops.2024.100480
ISSN 2666-9145/24

shares a similar structure to brain tissue with regard to the vasculature as well as the inflammatory microenvironment.[12] However, unlike the brain, the retina can be directly and repeatedly visualized, making it an ideal surrogate for monitoring neuronal changes in neurodegenerative disease.[10] Some evidence has been reported suggesting an association between retinal structural alterations and a diagnosis of MCI. Exploratory studies using optical coherence tomography angiography (OCTA) have reported alterations in the retinal capillary plexus vessel density (VD)[8,13,14] and attenuation of the retinal nerve fiber layer, but these results seem to be mixed.[13–17] Ultrawidefield (UWF) imaging is unique in that it captures a significantly larger area of the retina, largely unseen on OCTA and conventional fundus photography.[18] Therefore, this UWF technology allows more of the peripheral retina to be examined for possible pertinent biomarkers.[19] One pilot study has used UWF imaging to document peripheral drusen deposition longitudinally as well as peripheral vascular changes in individuals with AD over a 2-year period.[20] Specifically, this study found increased attenuation of peripheral retinal vasculature in individuals with AD.[20] This suggests that imaging of the peripheral retinal vascular network has value in monitoring the progression of neurodegenerative disease. One pilot cross sectional study has been published analyzing UWF images in MCI and found increased peripheral retinal arterial and venous thinning.[21] In this study, we aim to build on prior work to demonstrate the use of UWF imaging to characterize both the retinal and choroidal vasculature in a larger cohort of individuals with MCI compared with that of controls with normal cognition.

Methods

Duke Health Institutional Review Board (Pro00082598) approval was obtained. We adhered to the regulations outlined in the Health Insurance Portability and Accountability Act of 1996 and the principles of the World Medical Association Declaration of Helsinki. Before enrolling in the study, all participants or their legally authorized representatives provided written informed consent.

Study Participants

Study participants $>$ 50 years of age were enrolled from the Duke Memory Clinic. Individuals with a clinical diagnosis of MCI were diagnosed by Duke neurologists specializing in memory disorders after a review of symptomatology, cognitive evaluation, and adjunctive testing when available. Standardized criteria developed by the National Institute of Aging and the Alzheimer's Association were used to identify patients with MCI.[22] These criteria include the following: "concern regarding a change in cognition, objective evidence of impairment in one or more cognitive domain, preservation of independence in functional abilities, and not demented."[22] Duke neurologists also further classified each MCI patient as either amnestic MCI or nonamnestic MCI. Control participants were cognitively normal individuals who were recruited from the surrounding community, Duke clinics, and the Duke Alzheimer's Disease Prevention Registry of research volunteers with normal cognition. Participants from the Duke Alzheimer's Disease Prevention Registry were classified as cognitively normal after undergoing an extensive battery of neuropsychological testing. Participants who were not recruited from the Duke Alzheimer's Disease Prevention Registry were classified as cognitively normal after a review of cognitive evaluation completed at the time of the study visit and further medical record review when available.

Exclusion criteria included a history of glaucoma, retinal pathology, diabetes mellitus, uncontrolled hypertension, a spherical equivalent of <-6 or >6 diopters, and Snellen visual acuity worse than 20/40 as measured at the time of data collection. These criteria minimized confounding factors that might otherwise affect imaging and analysis of the retinal and choroidal vasculature. Participants completed a brief questionnaire assessing known ophthalmic and medical conditions. This information was subsequently confirmed through medical record review when available. The Mini-Mental State Examination (MMSE) was used for cognitive evaluation at the time of image acquisition. The 11-question MMSE is scored out of 30 total points and assesses individuals in 5 categories: orientation, registration, attention and calculation, recall, and language.[23]

Image Acquisition and Retinal Vessel Parameters

All images were obtained without pupillary dilation. Ultrawidefield images were obtained using a scanning laser ophthalmoscope (UWF-SLO) (California, Optos Inc). A standardized elliptical region of interest (ROI), from which the optic disc itself was excluded, was used for all images (Fig 1). The ROI was selected by studying a prior data set of UWF images. In this data set, the largest possible region that would consistently exclude eyelash artifacts was chosen. The posterior ROI was defined as a ring between 0 and 3 optic disc diameters from the optic disc boundary. It has a radius of 5.2 mm that corresponds to a field of view of $\sim$50°.

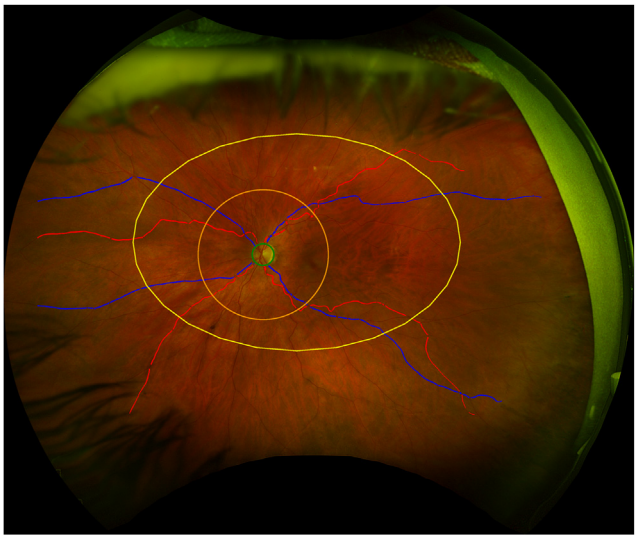

Figure 1. Schematic of the standard region of interest (ROI; yellow). This is further subdivided into the posterior ROI (between the green circle and the orange circle) and the midperipheral ROI (between the orange circle and the yellow circle). The posterior ROI is at $\sim$50° field of view (5.2 mm radius) and captures the optic disc and arcades. The midperipheral ROI is at $\sim$ 120° horizontal field of view (12.6 mm major axis) and $\sim$90° vertical field of view (8.5 mm minor axis) and contains the posterior edge of the vortex vein ampulla. The total area of the standard ROI is 319 mm^2. The annotated retinal vessel paths have been highlighted with arteries in red and veins in blue.

The midperipheral ROI is the remaining area of the standard ROI that is not included in the posterior ROI. Midperipheral ROI has a vertical field of view of ~ 90° and a minor axis of 8.5 mm. The total area of the standard ROI is 319 mm^2. Any images that were off-center, had artifacts interfering with the standard ROI (e.g., eyelashes or eyelids), reflections, or had blurred vessels, were excluded from the study.

Analysis of retinal vessel structure was performed using the VAMPIRE-UWF 2.0 (Vasculature Assessment Platform for Images of the Retina; Universities of Edinburgh and Dundee) software.[24] First, a trained masked operator (A.H.) was given a choice to include or exclude an image based on image quality (i.e., the presence of eyelashes and eyelids obstructing the view of retinal vasculature or the image is too blurred or of inadequate exposure to visualize the vessels). The operator then manually defined the boundaries of the optic disc and the location of the center of the fovea. Each image was automatically divided into 4 quadrants (superotemporal, inferotemporal, inferonasal, and superonasal). Boundaries of the quadrants were determined by a horizontal line crossing the center of the optic disc and the center of the fovea and another perpendicular to this line crossing the optic disc center. The software automatically generated a vessel map that detected the retinal vessels and classified them as arteries or veins. From this map, the operator selected the most prominent (i.e., widest) retinal artery and vein within each quadrant. Misclassified vessels could be manually corrected by the operator. The width of a selected vessel was measured at regular intervals along its vessel path, and robust regression was performed to determine the width gradient (which quantified the rate of thinning along the vessel path) and width intercept (the width of the vessel extrapolated to the center of the optic disc) shown in Figure 2. More negative width gradients represent an increased degree of peripheral thinning, whereas a less negative width gradient represents less peripheral thinning. Higher-width intercepts represent wider vessels, whereas lower-width intercepts represent thinner vessels.

Tortuosity quantifies how much a vessel twists and turns and was measured using tortuosity density due to its high correlation with human tortuosity grading.[25,26] Tortuosity density accounts for the total number of curves (separated by inflection points) within a smoothed vessel path as well as the total deviation of each curve from a straight path.[25] All path analysis variables (width gradient, width intercept, and tortuosity) are ROI independent. The fractal dimension quantifies how "space-filling" the vascular network is. Fractal dimensions of the detected retinal arteries and veins were automatically generated by the software through a multifractal approach in the standard, posterior, and midperipheral ROI.[27] A healthy retinal vasculature will have an optimum arrangement of vessels occupying the space in a way that provides the best blood supply and drainage to the entire retina. Deviation from this arrangement, reflected through either a higher fractal dimension (indicating that the vessels occupy more space) or a lower fractal dimension, suggests that some areas may be getting inefficient blood supply and drainage.

The choroid, which is visualized through the red channel of the UWF image (due to the ability of the red laser to penetrate the retinal pigment epithelium), was binarized using Niblack auto-local thresholding (Fig 3),[28] in a process comparable to the calculation of choroidal vascularity index (CVI) from OCT images.[29] Large vessel choroidal vascular density was calculated as the ratio between the area of choroidal vasculature compared with the ROI captured from an en face perspective. This is a novel parameter derived from UWF images that quantifies choroidal vascularity and was measured in the standard, posterior, and midperipheral ROIs.

Data Analysis

Retinal and choroidal vascular parameters from patients with MCI were compared with controls with normal cognition. A secondary analysis was conducted to compare amnestic MCI, nonamnestic MCI, and controls with normal cognition. The SAS/STAT software, Version 9.4 of the SAS System for Windows (2002-2012 SAS Institute Inc.), was used to perform statistical analysis. Data were reported for the nasal and temporal regions. The superonasal and inferonasal data were averaged to create the nasal region, whereas the superotemporal and inferotemporal data were averaged to create the temporal region. Demographic characteristics were compared with assess for possible confounders. The chi-square test was used to evaluate differences in sex, and the Wilcoxon rank sum test was used to assess differences in MMSE score and age. Generalized estimating equations, adjusted for age and sex, were then used to compare the imaging parameters between groups while accounting for the correlation between 2 eyes within the same study participant. All statistical tests were 2-sided. A P value of < 0.05 was considered statistically significant.

Results

We imaged 176 eyes from 88 MCI patients and 304 eyes from 152 control participants. Of these, 45 MCI eyes and 73 control eyes were excluded because of poor image quality/significant image artifact after manual review. Table 1 describes the demographics of the study population. Patients with MCI had lower MMSE scores ($P < 0.001$). MCI patients were similar to controls in age ($P = 0.155$). There was a greater percentage of male participants in the MCI group compared with controls ($P < 0.001$).

Table 2 and Table 3 show the differences in retinal vessel width gradient and retinal vessel width intercept, respectively, in the eyes of individuals with MCI compared with controls when controlling for age and sex. Average arterial and venous width gradients were less negative, representing decreased rates of vessel thinning, among individuals with MCI compared with that of controls ($P < 0.001$; $P = 0.027$). This held true when analyzing the arterial width gradient in the nasal and temporal areas of the retina ($P < 0.001$; $P = 0.026$) and when analyzing the venous width gradient in the nasal area ($P = 0.026$).

Average retinal arterial and venous width intercepts were smaller, representing thinner vessels, among individuals with MCI compared with controls ($P < 0.001$; $P = 0.017$). This held true when analyzing the arterial width intercept in the nasal and temporal areas of the retina ($P < 0.001$; $P = 0.001$) and when analyzing the venous width intercept in the nasal area ($P = 0.009$).

Table 4 shows the differences in large vessel choroidal vascular density in the eyes of individuals with MCI compared with controls. Large vessel choroidal vascular density was higher, indicating increased choroidal vascular density, in individuals with MCI compared with that of controls ($P = 0.025$). This held true when analyzing both the posterior and midperipheral ROI separately within the retina ($P = 0.026$, $P = 0.015$). There were no significant differences present in vessel tortuosity or fractal

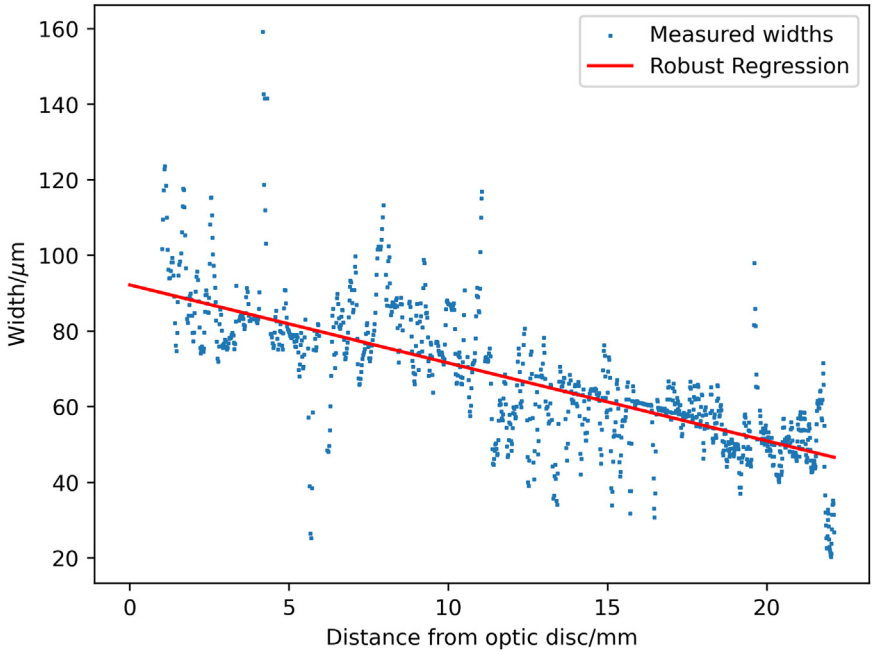

Figure 2. Regression analysis of a mild cognitive impairment eye comparing the retinal vessel width (μm) to the distance along the vessel path (mm). The line of best fit is used to calculate the width gradient and the y-intercept is used to calculate the width intercept.

dimension between MCI eyes and control eyes (Tables 5 and 6).

A subgroup analysis was conducted comparing MCI subgroups (amnestic MCI and nonamnestic MCI) with controls (Tables S7 and S8, available at www.ophthalmologyscience.org). Of the 131 MCI eyes, 98 were amnestic, and 33 were nonamnestic. For both retinal arteries as well as veins, the width gradient was less negative (i.e., decreased rates of vessel thinning) and the width intercept was lower (i.e., thinner vessels) in amnestic MCI compared with that of controls. In addition, large vessel choroidal vascular density was increased in eyes with amnestic MCI compared with those of controls. Nasal arterial width gradient was less negative in nonamnestic MCI compared with controls. Average arterial and nasal arterial width intercepts were lower in nonamnestic MCI compared with that of controls. There was no evidence of differences in large vessel choroidal vascular density among nonamnestic MCI and controls. Overall fractal dimension in the midperipheral ROI was higher in nonamnestic MCI compared with that of controls.

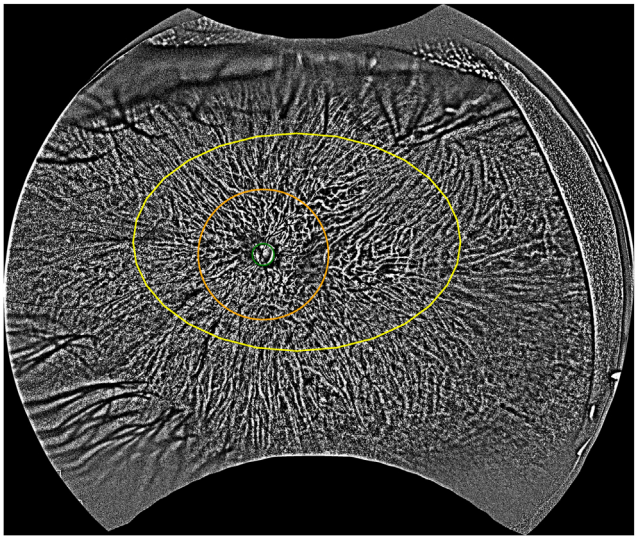

Figure 3. The segmentation of the choroidal vasculature (shown in white) of a mild cognitive impairment patient. This was produced by applying Niblack auto-local thresholding to the red channel of an ultrawidefield image.

Table 1. Demographics in Eyes of Individuals with MCI vs. Controls

Variable	Statistic	MCI	Controls	*P* Value*
Age	N	82	133	
	Mean (SD)	70.7 (8.5)	70.4 (6.6)	0.155
	Minimum, median, maximum	44, 73, 84	52, 70, 89	
MMSE	N	82	133	
	Mean (SD)	27.3 (2.5)	29.7 (0.7)	**< 0.001**
	Minimum, median, maximum	19, 28, 30	25, 30, 30	
Male sex	N (%)	40 (48.8)	30 (22.6)	**< 0.001**

P value for sex based on chi-square test.
MCI = mild cognitive impairment; MMSE = Mini-Mental State Examination; SD = standard deviation.
**P* value for age and MMSE based on Wilcoxon rank sum test. Values of statistical significance are bolded.

Table 2. Retinal Vessel Width Gradient (μm/mm) in Eyes of Individuals with MCI vs. Controls

Variable	Statistic	MCI	Controls	*P* Value*
Average arteriolar width gradient	N	131	230	
	Mean (SD)	−2.46 (0.93)	−2.83 (0.96)	**< 0.001**
	Minimum, median, maximum	−4.43, −2.45, 0.73	−6.82, −2.83, −0.34	
Nasal arteriolar width gradient	N	131	230	
	Mean (SD)	−2.14 (1.32)	−2.63 (1.43)	**< 0.001**
	Minimum, median, maximum	−5.57, −2.25, 3.56	−10.03, −2.55, 1.01	
Temporal arteriolar width gradient	N	131	230	
	Mean (SD)	−2.78 (1.07)	−3.03 (0.10)	**0.026**
	Minimum, median, maximum	−5.40, −2.62, 0.31	−5.94, −3.08, 0.68	
Average venular width gradient	N	131	230	
	Mean (SD)	−3.74 (1.05)	−3.97 (0.99)	**0.027**
	Minimum, median, maximum	−7.32, −3.63, −1.59	−7.65, −3.92, −1.68	
Nasal venular width gradient	N	131	230	
	Mean (SD)	−3.40 (1.49)	−3.75 (1.53)	**0.026**
	Minimum, median, maximum	−9.25, −3.23, −0.23	−9.25, −3.54, −0.57	
Temporal venular width gradient	N	131	230	
	Mean (SD)	−4.08 (1.12)	−4.19 (0.97)	0.294
	Minimum, median, maximum	−8.56, −3.97, −1.30	−7.46, −4.11, −1.98	

MCI = mild cognitive impairment; SD = standard deviation.
**P* value based on regression analysis using generalized estimating equations to account for including both eyes of each patient in the analysis and adjusted for age and sex. Values of statistical significance are bolded.

Discussion

This is a novel cross sectional study that analyzes UWF images to evaluate retinal vessel width intercept, arterial and venous fractal dimension, and large vessel choroidal vascular density in individuals with MCI. In MCI participants, we observed thinner arteries and veins which both attenuated less when traveling toward the periphery compared with controls. Additionally, we observed increased large vessel choroidal vascular density in the eyes of MCI patients compared with controls.

The retinal vessel width gradient and width intercept are novel metrics that quantify the rate of vessel tapering that occurs as the vessel moves from the optic disc to the peripheral retina and the width of the vessel extrapolated to the center of the optic disc, respectively. To accurately characterize the differences between retinal vessels in UWF images of the eyes of MCI individuals compared with the

Table 3. Retinal Vessel Width Intercept (μm) in Eyes of Individuals with MCI vs. Controls

Variable	Statistic	MCI	Controls	*P* Value*
Average arteriolar width intercept	N	131	230	
	Mean (SD)	91.68 (12.17)	99.68 (15.27)	**< 0.001**
	Minimum, median, maximum	63.28, 92.12, 116.63	60.40, 99.15, 159.63	
Nasal arteriolar width intercept	N	131	230	
	Mean (SD)	80.15 (14.45)	88.22 (18.41)	**< 0.001**
	Minimum, median, maximum	41.04, 79.80, 132.67	41.17, 85.83, 167.21	
Temporal arteriolar width intercept	N	131	230	
	Mean (SD)	103.22 (15.15)	111.15 (16.61)	**0.001**
	Minimum, median, maximum	59.24, 103.46, 132.53	53.51, 111.58, 152.05	
Average venular width intercept	N	131	230	
	Mean (SD)	124.28 (17.27)	129.45 (16.66)	**0.017**
	Minimum, median, maximum	91.42, 125.29, 171.81	82.57, 128.92, 178.14	
Nasal venular width intercept	N	131	230	
	Mean (SD)	108.23 (19.58)	114.51 (20.19)	**0.009**
	Minimum, median, maximum	72.28, 104.58, 183.02	70.68, 113.72, 203.90	
Temporal venular width intercept	N	131	230	
	Mean (SD)	140.32 (19.85)	144.39 (18.92)	0.132
	Minimum, median, maximum	95.33, 139.73, 185.52	88.85, 143.90, 196.43	

MCI = mild cognitive impairment; SD = standard deviation.
**P* value based on regression analysis using generalized estimating equations to account for including both eyes of each patient in the analysis and adjusted for age and sex. Values of statistical significance are bolded.

Table 4. Large Vessel Choroidal Vascular Density in Eyes of Individuals with MCI vs. Controls

Variable	Statistic	MCI	Controls	*P* Value*
Large vessel choroidal vascular density in standard ROI	N	131	230	
	Mean (SD)	0.297 (0.025)	0.288 (0.025)	**0.025**
	Minimum, median, maximum	0.189, 0.300, 0.345	0.204, 0.291, 0.347	
Large vessel choroidal vascular density in posterior ROI	N	131	230	
	Mean (SD)	0.302 (0.026)	0.294 (0.027)	**0.026**
	Minimum, median, maximum	0.194, 0.306, 0.355	0.197, 0.295, 0.370	
Large vessel choroidal vascular density in midperipheral ROI	N	131	230	
	Mean (SD)	0.295 (0.026)	0.286 (0.025)	**0.015**
	Minimum, median, maximum	0.188, 0.299, 0.346	0.209, 0.288, 0.347	

MCI = mild cognitive impairment; ROI = region of interest; SD = standard deviation.
**P* value based on regression analysis using generalized estimating equations to account for including both eyes of each patient in the analysis and adjusted for age and sex. Values of statistical significance are bolded.

eyes of cognitively normal individuals, it is important to interpret these metrics together, which has not yet been previously reported. We found the width gradient for retinal arteries and veins to be less negative, whereas the width intercept was smaller in MCI individuals compared with that of controls. This suggests that, in MCI, more posterior retinal vessels are narrower and that those narrow vessels undergo less attenuation as they move toward the periphery compared with controls. Prior works using OCTA in the macula of MCI individuals have reported mixed results on retinal vessel density when compared with that of controls with some studies reporting decreased vessel density[13,14] and others reporting no changes.[8,30] The mixed literature on MCI biomarkers in OCTA studies highlights the importance of incorporating UWF imaging for biomarker identification.

Furthermore, UWF imaging may have the potential to help track MCI disease progression to AD. Our MCI cohort demonstrated that the overall width of the retinal arteries and veins was less attenuated as they moved along their vessel path toward the periphery compared with that of controls. However, width gradient analysis in AD patients has been reported to exhibit increased attenuation of vessels toward the periphery.[20] Given our results of thinner retinal vasculature posteriorly with less attenuation peripherally in MCI eyes, it is possible that the vessel attenuation occurs first more posteriorly in the macular region, which has a higher metabolic demand.[31] We hypothesize that this attenuation could then progress to the periphery as the AD pathology transitions from MCI to AD. Future work could analyze the width gradients in the macular and peripheral regions of the retina to further elucidate this theory.

Table 5. Retinal Vessel Tortuosity in Eyes of Individuals with MCI vs. Controls

Variable	Statistic	MCI	Controls	*P* Value*
Average arteriolar tortuosity	N	131	230	
	Mean (SD)	0.029 (0.038)	0.027 (0.027)	0.706
	Minimum, median, maximum	0.001, 0.018, 0.320	0.002, 0.020, 0.169	
Nasal arteriolar tortuosity	N	131	230	
	Mean (SD)	0.014 (0.028)	0.014 (0.028)	0.907
	Minimum, median, maximum	0.000, 0.003, 0.193	0.000, 0.004, 0.185	
Temporal arteriolar tortuosity	N	131	230	
	Mean (SD)	0.038 (0.056)	0.035 (0.036)	0.744
	Minimum, median, maximum	0.002, 0.020, 0.483	0.002, 0.025, 0.267	
Average venular tortuosity	N	131	230	
	Mean (SD)	0.041 (0.048)	0.038 (0.040)	0.621
	Minimum, median, maximum	0.001, 0.032, 0.374	0.003, 0.026, 0.250	
Nasal venular tortuosity	N	131	230	
	Mean (SD)	0.022 (0.083)	0.016 (0.028)	0.680
	Minimum, median, maximum	0.000, 0.006, 0.933	0.000, 0.006, 0.227	
Temporal venular tortuosity	N	131	230	
	Mean (SD)	0.053 (0.061)	0.051 (0.061)	0.646
	Minimum, median, maximum	0.001, 0.032, 0.477	0.002, 0.032, 0.398	

MCI = mild cognitive impairment; SD = standard deviation.
**P* value based on regression analysis using generalized estimating equations to account for including both eyes of each patient in the analysis and adjusted for age and sex.

Table 6. Fractal Dimension in Eyes of Individuals with MCI vs. Controls

Variable	Statistic	MCI	Controls	*P* Value*
Arterial fractal dimension in standard ROI	N	131	230	
	Mean (SD)	1.089 (0.051)	1.099 (0.040)	0.274
	Minimum, median, maximum	0.862, 1.102, 1.150	0.890, 1.111, 1.157	
Arterial fractal dimension in posterior ROI	N	131	230	
	Mean (SD)	1.318 (0.063)	1.331 (0.059)	0.285
	Minimum, median, maximum	1.062, 1.331, 1.410	1.072, 1.337, 1.439	
Arterial fractal dimension in midperipheral ROI	N	131	230	
	Mean (SD)	1.039 (0.061)	1.045 (0.047)	0.706
	Minimum, median, maximum	0.746, 1.056, 1.124	0.844, 1.059, 1.117	
Venule fractal dimension in standard ROI	N	131	230	
	Mean (SD)	1.086 (0.031)	1.084 (0.028)	0.828
	Minimum, median, maximum	0.963, 1.090, 1.152	0.957, 1.086, 1.143	
Venular fractal dimension in posterior ROI	N	131	230	
	Mean (SD)	1.298 (0.051)	1.303 (0.050)	0.532
	Minimum, median, maximum	1.114, 1.303, 1.395	1.077, 1.311, 1.417	
Venular fractal dimension in midperipheral ROI	N	131	230	
	Mean (SD)	1.031 (0.038)	1.025 (0.037)	0.459
	Minimum, median, maximum	0.914, 1.034, 1.112	0.871, 1.027, 1.116	
Fractal dimension in standard ROI	N	131	230	
	Mean (SD)	1.158 (0.025)	1.161 (0.020)	0.442
	Minimum, median, maximum	1.055, 1.163, 1.199	1.087, 1.165, 1.195	
Fractal dimension in posterior ROI	N	131	230	
	Mean (SD)	1.447 (0.035)	1.454 (0.038)	0.261
	Minimum, median, maximum	1.345, 1.451, 1.503	1.284, 1.458, 1.532	
Fractal dimension in midperipheral ROI	N	131	230	
	Mean (SD)	1.114 (0.030)	1.113 (0.028)	0.756
	Minimum, median, maximum	1.010, 1.118, 1.166	1.027, 1.118, 1.159	

P value based on the test of the difference between means using generalized estimating equations to adjust for the correlation between eyes of the same subject and adjusted for age and sex.
MCI = mild cognitive impairment; ROI = region of interest; SD = standard deviation.
**P* value based on regression analysis using generalized estimating equations to account for including both eyes of each patient in the analysis and adjusted for age and sex.

Our subgroup analysis demonstrated more retinal vascular findings in our amnestic MCI subgroup than in our nonamnestic MCI subgroup when compared with controls. Amnestic MCI is characterized by episodic memory impairment and poses an increased yearly risk of progression to AD compared with nonamnestic MCI.[32] Robbins et al[33] found decreased macular perfusion density in amnestic MCI but reported no retinal vessel findings in nonamnestic MCI when compared with controls. These results are echoed in our findings. We report retinal arterial and venous thinning and decreased peripheral vessel attenuation as well as increased large vessel choroidal vascular density in amnestic MCI. However, in our nonamnestic MCI cohort, we only found arterial thinning and decreased peripheral arterial attenuation in the nasal region. No retinal venous changes or choroidal changes were observed in the nonamnestic MCI subgroup. These results suggest that amnestic MCI may be more susceptible to or may be associated with retinal vascular abnormalities. UWF imaging may be useful in the earlier identification of amnestic MCI and in the differentiation of amnestic from nonamnestic MCI.

Of note, Pead et al[21] found increased peripheral retinal vessel attenuation (more negative width gradient) in MCI individuals compared with controls. This difference could be due to different sample sizes between the 2 studies. Our study analyzed 131 MCI eyes compared with 45 MCI eyes in Pead et al,[21] and, as such, our study may be more robust and less susceptible to the effects of MCI subtype. As discussed above, prior work has reported retinal vessel differences among eyes with amnestic MCI and nonamnestic MCI.[33] Our cohort consisted of 98 amnestic MCI eyes (74.8%) which could be reflected in our findings. Pead et al[21] did not conduct any subgroup analyses. Currently, there are no other works analyzing the retinal vessel width gradient in MCI. Pead et al[21] also reported an increased superonasal retinal arterial tortuosity in MCI compared with controls. This difference could be partly attributed to the different tortuosity algorithms used between studies with Pead et al[21] using curvature-integral methods, whereas we used tortuosity density. Our study did not find any evidence of significant differences in arterial or venous tortuosity between MCI and controls.

Our UWF study reports increased large vessel choroidal vascular density in MCI compared with that of controls. This is a novel parameter that aims to quantify the en face vascular density of the largest vessels of the choroid on a UWF image. This calculation was designed to mimic CVI measured on macular OCT images and uses the same thresholding algorithm for binarization.[29] Of note, a prior study reported decreased CVI in individuals with MCI.[34] Although both OCT CVI and UWF large vessel choroidal

vascular density measurements serve to characterize the choroid, the cross sectional macular view offered by OCT provides different information than the en face viewpoint offered by UWF-scanning laser ophthalmoscope imaging. Choroidal vascularity index calculated from OCT does not account for the midperipheral or peripheral retina but, instead, is often calculated from a 1.5 mm area centered on the fovea,[34] whereas large vessel choroidal vascular density offers no separation of the choroidal layers and focuses on the large and medium-sized vessels. Therefore, the 2 metrics are not necessarily expected to correlate because they measure different choroidal features and regions. Other studies analyzing the choroid have reported decreased subfoveal choroidal thickness in both MCI[35] and AD when compared with that of controls.[36,37] However, it should be noted that subfoveal choroidal thickness is more subject to daily fluctuations and other variables than CVI.[29] Of note, our subgroup analysis demonstrated increased large vessel choroidal vascular density only in the eyes of amnestic MCI participants. This novel assessment of the midperipheral choroidal region, outside the macular region, deserves further investigation to determine its utility.

Although our study found no difference in arterial or venous fractal dimension in MCI, 1 prior paper has reported decreased fractal dimension in participants with cognitive impairment with no dementia.[38] Ong et al[38] used a nonmydriatic digital camera to image the retina and imaged a significantly smaller area than we did in our study ($< 50°$ vs. $\sim 120°$), which could contribute to the differences seen.

When interpreting the results of our study, there are important points to consider. Although all neurological diagnoses were made by expert neurologists trained in memory disorders, MCI is traditionally a clinical diagnosis. As such, we did not confirm whether participants had positive cerebrospinal fluid or MRI biomarkers consistent with MCI. Additionally, not all control participants were evaluated by neurologists to ensure that they were cognitively normal. However, all control individuals did undergo MMSE testing on the day of study entry and also medical record review when available. Furthermore, given the novel nature and limited prior work on the retinal imaging parameters reported herein, we limited confounding variables with our prespecified exclusion criteria including uncontrolled hypertension, diabetes mellitus, glaucoma, and vitreoretinal pathology. By limiting our study participants, these findings may not necessarily be representative of the general population where these confounders frequently occur. As we better understand differences in retinal imaging parameters in more defined cohorts, future studies will then be designed to determine the combined effect of these confounding variables on the retinal parameters measured. Because of the exploratory nature of this study, correction for multiple associations was not performed. As such, there may be an increased risk of type 1 error in this study. The Optos device software used for UWF imaging uses a standard eye model to adjust for the curvature of the retina, and, as such, there could be inaccuracies in metrics derived from participants with irregularly shaped eyes. However, our paper mitigates this by excluding patients with spherical equivalents > 6 and < -6. Additionally, the use of the binarization threshold on red channel UWF images to analyze the choroid is a process that has not yet been validated. Future studies to further assess the utility of choroidal vascular density as an imaging metric and potential biomarker are needed. Finally, although our ROI is equally as large as the largest ROI in prior work analyzing retinal images in MCI,[21] it does not encompass the entire peripheral retina. This approach was selected to maintain a standard ROI across all images while also minimizing the number of images rejected due to eyelash and eyelid artifacts and occlusion. Nevertheless, using a standard ROI only affects the fractal dimension and efCVI measurements because the vessel paths measured for width gradient, width intercept, and tortuosity analysis extend beyond this ROI and further into the periphery.

In conclusion, we found that MCI patients had thinner retinal vasculature in both the retinal arteries and veins when compared with controls. Additionally, these thinner retinal arteries and veins attenuated less when traveling toward the periphery, perhaps because they were more attenuated posteriorly than controls. MCI patients also had increased large vessel choroidal vascular density. These findings suggest that UWF images may have added value in the search for clinically relevant retinal biomarkers as we strive to more accurately and easily identify those with MCI and those at risk of deteriorating cognitive health.

Footnotes and Disclosures

Originally received: November 17, 2023.
Final revision: January 22, 2024.
Accepted: January 23, 2024.
Available online: February 1, 2024.Manuscript no. XOPS-D-23-00300R2.

[1] Department of Ophthalmology, Duke University School of Medicine, Durham, North Carolina.

[2] iMIND Research Group, Duke University School of Medicine, Durham, North Carolina.

[3] Department of Neurology, Duke University School of Medicine, Durham, North Carolina.

[4] Centre for Clinical Brain Science, University of Edinburgh, Scotland, United Kingdom.

*S.J. and A.H. shared the first authorship.

**D.S.G. and S.F. shared the senior authorship.

Disclosure(s):

All authors have completed and submitted the ICMJE disclosures form.

The author(s) have made the following disclosure(s):

A.T.: Support − Optos plc.

T.J.M.: Support − Alzheimer's Drug Discovery Foundation; Participation on an Advisory Board − Scientific Advisory Board for Alzheimer's Drug Discovery Foundation, Scientific Advisory Board for Moorfields Eye Charity; Other financial or non-financial interests − Scientific Advisor to Eye to the Future, a UK-based medical software company.

S.F.: Research support − Genentech, Optos; Patent royalties − Alcon; Consulting fees − Glaukos, Alimera, Bausch Surgical, Apellis; Receipt of equipment − Optos (Loaner equipment).

The other authors have no proprietary or commercial interest in any materials discussed in this article.

This work was supported in part by Optos Inc.

The scanning laser ophthalmoscope (SLO), California, used in this study is a loaner from Optos Inc., Marlborough, MA. The sponsor or funding organization had no role in the design or conduct of the research.

HUMAN SUBJECTS: Human subjects were included in this study. Duke Health Institutional Review Board (Pro00082598) approval was obtained. All research adhered to the tenets of the Declaration of Helsinki. All participants provided informed consent.

No animal subjects were used in this study.

Author Contributions:

Conception and design: Joseph, Threlfall, MacGillivray, Grewal, Fekrat

Data collection: Joseph, Haystead, Threlfall, MacGillivray, Stinnett

Analysis and interpretation: Joseph, Haystead, Robbins, Threlfall, MacGillivray, Stinnett, Grewal, Fekrat

Obtained funding: Fekrat

Overall responsibility: Joseph, Haystead, Robbins, Threlfall, MacGillivray, Stinnett, Grewal, Fekrat

Abbreviations and Acronyms:
AD = Alzheimer dementia; **CVI** = choroidal vascularity index; **MCI** = mild cognitive impairment; **MMSE** = Mini-Mental State Examination; **OCTA** = optical coherence tomography angiography; **ROI** = region of interest; **UWF** = ultrawidefield.

Keywords:
Diagnostic imaging, MCI, Retinal vasculature, Ultrawidefield fundus imaging.

Correspondence:
Suzanna Joseph, Department of Ophthalmology, Duke University School of Medicine, Durham, North Carolina. E-mail: Suzanna.joseph@duke.edu.

References

1. Sanford AM. Mild cognitive impairment. *Clin Geriatr Med*. 2017;33:325−337. https://doi.org/10.1016/j.cger.2017.02.005.
2. Lopez OL. Mild cognitive impairment. *Continuum (Minneap Minn)*. 2013;19:411−424. https://doi.org/10.1212/01.CON.0000429175.29601.97.
3. Petersen RC, Smith GE, Waring SC, et al. Mild cognitive impairment: clinical characterization and outcome. *Arch Neurol*. 1999;56:303−308. https://doi.org/10.1001/archneur.56.3.303.
4. Tierney MC, Szalai JP, Snow WG, et al. Prediction of probable Alzheimer's disease in memory-impaired patients: a prospective longitudinal study. *Neurology*. 1996;46:661−665. https://doi.org/10.1212/wnl.46.3.661.
5. Tangalos EG, Petersen RC. Mild cognitive impairment in geriatrics, 20180821 *Clin Geriatr Med*. 2018;34:563−589. https://doi.org/10.1016/j.cger.2018.06.005.
6. Giau VV, Bagyinszky E, An SSA. Potential fluid biomarkers for the diagnosis of mild cognitive impairment. *Int J Mol Sci*. 2019;20:4149. https://doi.org/10.3390/ijms20174149.
7. Simrén J, Leuzy A, Karikari TK, et al. The diagnostic and prognostic capabilities of plasma biomarkers in Alzheimer's disease. *Alzheimers Dement*. 2021;17:1145−1156. https://doi.org/10.1002/alz.12283.
8. Yoon SP, Grewal DS, Thompson AC, et al. Retinal microvascular and neurodegenerative changes in Alzheimer's disease and mild cognitive impairment compared with control participants. *Ophthalmol Retina*. 2019;3:489−499. https://doi.org/10.1016/j.oret.2019.02.002.
9. Robbins CB, Grewal DS, Thompson AC, et al. Identifying peripapillary radial capillary plexus alterations in Parkinson's disease using OCT angiography. *Ophthalmol Retina*. 2022;6:29−36. https://doi.org/10.1016/j.oret.2021.03.006.
10. Snyder PJ, Alber J, Alt C, et al. Retinal imaging in Alzheimer's and neurodegenerative diseases. *Alzheimers Dement*. 2021;17:103−111. https://doi.org/10.1002/alz.12179.
11. Jiang H, Delgado S, Liu C, et al. In vivo characterization of retinal microvascular network in multiple sclerosis. *Ophthalmology*. 2016;123:437−438. https://doi.org/10.1016/j.ophtha.2015.07.026.
12. London A, Benhar I, Schwartz M. The retina as a window to the brain-from eye research to CNS disorders. *Nat Rev Neurol*. 2013;9:44−53. https://doi.org/10.1038/nrneurol.2012.227.
13. Wang X, Zhao Q, Tao R, et al. Decreased retinal vascular density in Alzheimer's disease (AD) and mild cognitive impairment (MCI): an optical coherence tomography angiography (OCTA) study. *Front Aging Neurosci*. 2020;12:572484. https://doi.org/10.3389/fnagi.2020.572484.
14. Wu J, Zhang X, Azhati G, et al. Retinal microvascular attenuation in mental cognitive impairment and Alzheimer's disease by optical coherence tomography angiography. *Acta Ophthalmol*. 2020;98:e781−e787. https://doi.org/10.1111/aos.14381.
15. Santos CY, Johnson LN, Sinoff SE, et al. Change in retinal structural anatomy during the preclinical stage of Alzheimer's disease. *Alzheimers Dement (Amst)*. 2018;10:196−209. https://doi.org/10.1016/j.dadm.2018.01.003.
16. Sánchez D, Castilla-Marti M, Marquié M, et al. Evaluation of macular thickness and volume tested by optical coherence tomography as biomarkers for Alzheimer's disease in a memory clinic. *Sci Rep*. 2020;10:1580. https://doi.org/10.1038/s41598-020-58399-4.
17. Knoll B, Simonett J, Volpe NJ, et al. Retinal nerve fiber layer thickness in amnestic mild cognitive impairment: case-control study and meta-analysis. *Alzheimers Dement (Amst)*. 2016;4:85−93. https://doi.org/10.1016/j.dadm.2016.07.004.
18. Kumar V, Surve A, Kumawat D, et al. Ultra-wide field retinal imaging: A wider clinical perspective. *Indian J Ophthalmol*. 2021;69:824−835. https://doi.org/10.4103/ijo.IJO_1403_20.
19. Quinn N, Csincsik L, Flynn E, et al. The clinical relevance of visualising the peripheral retina. *Prog Retin Eye Res*. 2019;68:83−109. https://doi.org/10.1016/j.preteyeres.2018.10.001.
20. Csincsik L, MacGillivray TJ, Flynn E, et al. Peripheral retinal imaging biomarkers for Alzheimer's disease: a pilot study. *Ophthal Res*. 2018;59:182−192. https://doi.org/10.1159/000487053.
21. Pead E, Thompson AC, Grewal DS, et al. Retinal vascular changes in Alzheimer's dementia and mild cognitive impairment: a pilot study using ultra-widefield imaging. *Transl Vis Sci Technol*. 2023;12:13. https://doi.org/10.1167/tvst.12.1.13.
22. Albert MS, DeKosky ST, Dickson D, et al. The diagnosis of mild cognitive impairment due to Alzheimer's disease: recommendations from the National Institute on Aging-Alzheimer's Association workgroups on diagnostic guidelines for Alzheimer's disease. *Alzheimers Dement*. 2011;7:270−279. https://doi.org/10.1016/j.jalz.2011.03.008.

23. Ismail Z, Rajji TK, Shulman KI. Brief cognitive screening instruments: an update. *Int J Geriatr Psychiatry*. 2010;25:111−120. https://doi.org/10.1002/gps.2306.
24. Pellegrini E, Robertson G, Trucco E, et al. Blood vessel segmentation and width estimation in ultra-wide field scanning laser ophthalmoscopy. *Biomed Opt Express*. 2014;5:4329−4337. https://doi.org/10.1364/BOE.5.004329.
25. Grisan E, Foracchia M, Ruggeri A. A novel method for the automatic evaluation of retinal vessel tortuosity. In: *Proceedings of the 25th Annual International Conference of the IEEE Engineering in Medicine and Biology Society (IEEE Cat No03CH37439). Cancun*. Mexico: IEEE; 2003:866−869. https://doi.org/10.1109/IEMBS.2003.1279902.
26. Lisowska A, Annunziata R, Loh GK, et al. *An experimental assessment of five indices of retinal vessel tortuosity with the RET-TORT public dataset. 2014 36th Annual International Conference of the IEEE Engineering in Medicine and Biology Society*. Chicago, IL: IEEE; 2014:5414−5417. https://doi.org/10.1109/EMBC.2014.6944850.
27. Stosić T, Stosić BD. Multifractal analysis of human retinal vessels. *IEEE Trans Med Imaging*. 2006;25:1101−1107. https://doi.org/10.1109/tmi.2006.879316.
28. Niblack W. *An Introduction to Digital Image Processing*. Englewood Cliffs, NJ: Prentice Hall; 1986.
29. Agrawal R, Gupta P, Tan KA, et al. Choroidal vascularity index as a measure of vascular status of the choroid: measurements in healthy eyes from a population-based study. *Sci Rep*. 2016;6:21090. https://doi.org/10.1038/srep21090.
30. Hemesath A, Kundu A, Allen A, et al. Longitudinal retinal and choroidal findings in individuals with mild cognitive impairment compared to controls with normal cognition. 2023.
31. Joyal JS, Gantner ML, Smith LEH. Retinal energy demands control vascular supply of the retina in development and disease: the role of neuronal lipid and glucose metabolism. *Prog Retin Eye Res*. 2018;64:131−156. https://doi.org/10.1016/j.preteyeres.2017.11.002.
32. Mitchell AJ, Shiri-Feshki M. Rate of progression of mild cognitive impairment to dementia − meta-analysis of 41 robust inception cohort studies. *Acta Psychiatr Scand*. 2009;119:252−265. https://doi.org/10.1111/j.1600-0447.2008.01326.x.
33. Robbins CB, Akrobetu D, Ma JP, et al. Assessment of retinal microvascular alterations in individuals with amnestic and nonamnestic mild cognitive impairment using optical coherence tomography angiography. *Retina*. 2022;42:1338−1346. https://doi.org/10.1097/iae.0000000000003458.
34. Robbins CB, Grewal DS, Thompson AC, et al. Choroidal structural analysis in Alzheimer disease, mild cognitive impairment, and cognitively healthy controls. *Am J Ophthalmol*. 2021;223:359−367. https://doi.org/10.1016/j.ajo.2020.09.049.
35. Bulut M, Yaman A, Erol MK, et al. Choroidal thickness in patients with mild cognitive impairment and Alzheimer's type dementia. *J Ophthalmol*. 2016;2016:7291257. https://doi.org/10.1155/2016/7291257.
36. Chan VTT, Sun Z, Tang S, et al. Spectral-domain OCT measurements in Alzheimer's disease: a systematic review and meta-analysis. *Ophthalmology*. 2019;126:497−510. https://doi.org/10.1016/j.ophtha.2018.08.009.
37. Trebbastoni A, Marcelli M, Mallone F, et al. Attenuation of choroidal thickness in patients with Alzheimer disease: evidence from an Italian prospective study. *Alzheimer Dis Assoc Disord*. 2017;31:128−134. https://doi.org/10.1097/wad.0000000000000176.
38. Ong YT, Hilal S, Cheung CY, et al. Retinal vascular fractals and cognitive impairment. *Dement Geriatr Cogn Dis Extra*. 2014;4:305−313. https://doi.org/10.1159/000363286.